Techno-economic performances and life cycle greenhouse gas emissions of various ammonia production pathways including conventional, carbon-capturing, nuclear-powered, and renewable production

Journal:	*Green Chemistry*
Manuscript ID	GC-ART-03-2022-000843.R1
Article Type:	Paper
Date Submitted by the Author:	28-Apr-2022
Complete List of Authors:	Lee, Kyuha; Argonne National Laboratory, Energy Systems Division Liu, Xinyu; Argonne National Laboratory, Energy Systems Division Vyawahare, Pradeep; Argonne National Laboratory, Energy Systems Division Sun, Pingping; Argonne National Laboratory, Energy Systems Division ELGOWAINY, Amgad; Argonne National Laboratory, Energy Systems Division Wang, Michael; Argonne National Laboratory, Energy Systems Division

SCHOLARONE™
Manuscripts

Techno-economic performances and life cycle greenhouse gas emissions of various ammonia production pathways including conventional, carbon-capturing, nuclear-powered, and renewable production

Kyuha Lee,* Xinyu Liu, Pradeep Vyawahare, Pingping Sun, Amgad Elgowainy and Michael Wang

Ammonia (NH_3) is conventionally produced using fossil natural gas (NG) for hydrogen production through steam reformation, and synthesis in Haber-Bosch (HB) process. Conventional ammonia global production contributes to more than 420 million tons of CO_2 emissions annually. In this work, we investigated the techno-economics and well-to-plant-gate (WTG) greenhouse gas (GHG) emissions of conventional NG-based, carbon-capturing, nuclear-powered, and renewable ammonia production by developing engineering process model for each. Carbon-capturing ammonia refers to the NG-based ammonia produced while capturing CO_2 and transporting it via pipelines for storage or utilization. Nuclear-powered and renewable ammonia represent alternative ammonia production through water electrolysis, air separation, and HB processes using carbon-free energy sources. Nuclear and renewable energy sources are assumed to be used for nuclear-powered and renewable ammonia production, respectively. Sensitivity analyses are performed for CO_2 pipeline transport distances, potential carbon capture tax credits, and clean H_2 production cost. Carbon-capturing ammonia reduces WTG GHG emissions by 55–70% compared to conventional NG-based ammonia. Nuclear-powered and renewable ammonia almost eliminate GHG emissions since energy supply is either zero carbon or near-zero carbon. However, when \$4.16–\$4.83/kg is assumed for clean H_2 production cost using state-of-the-art electrolysis technologies, the levelized costs of nuclear-powered and renewable ammonia are calculated at \$0.92–\$1.06 per kg NH_3, which are approximately four times higher than the conventional NG-based ammonia production cost. The cost of CO_2 emissions avoidance is estimated in the range of \$266–\$318 per metric ton of CO_2 for nuclear-powered and renewable ammonia. The clean H_2 production cost is the major contributor to the levelized costs of nuclear-powered and renewable ammonia production. A lower clean H_2 production cost near \$1/kg H_2 is required for nuclear-powered and renewable ammonia production to be cost-competitive with conventional NG-based ammonia production.

Introduction

Ammonia is one of the major consumers of fossil energy.[1] Currently, more than 70% of feedstock used for global ammonia production is natural gas (NG),[2] while domestic ammonia production in the United States is predominantly from NG. Ammonia is produced via the Haber-Bosch (HB) process from nitrogen and hydrogen, which is conventionally produced through the steam methane reforming (SMR) of NG. Globally, 43% of annual hydrogen production, which corresponds to 31.5 million metric tons (MT), was used for ammonia production in 2018.[1] The production of ammonia has increased significantly in the past half-century due to its extensive use in nitrogen fertilizers for crop growth.[3] The world ammonia production in 2020 was more than 180 million MT. In the United States, ammonia production increased by 37% from 2016 to 2020 to reach 14 million MT, mainly due to the low cost of NG.[4,5]

Due to its massive production scale, ammonia industry consumes more energy and emits more greenhouse gases (GHGs) than other large-volume chemical industries such as ethylene, propylene, and methanol.[6] Ammonia production accounts for 2% of global fossil energy use and 1.2% of global GHG emissions, which correspond to approximately 420 million MT of CO_2 equivalent (CO_2e) annually.[2,7]

As part of the effort to achieve a decarbonized society, several alternative ammonia production pathways have been studied. One of the pathways is to synthesize ammonia from carbon-free sources including water, air, and zero carbon or near-zero carbon electricity such as solar, wind, and nuclear power.[3,8–10] The ammonia produced via such a pathway is called "green" ammonia. On the other hand, conventional ammonia produced from fossil resources is referred to as "grey" ammonia. Another pathway to reduce the carbon intensity of ammonia production is to capture and utilize CO_2 emitted from the conventional production processes. The captured CO_2 is pressurized and transported via pipelines to consumers for various CO_2 applications such as CO_2-enhanced oil recovery (EOR). Ammonia produced via this pathway is called "blue" ammonia.[11,12]

Considering the current applications of ammonia, carbon-neutral ammonia can contribute to the decarbonization of the agricultural

Systems Assessment Center, Energy Systems Division, Argonne National Laboratory, USA, E-mail: kyuha.lee@anl.gov
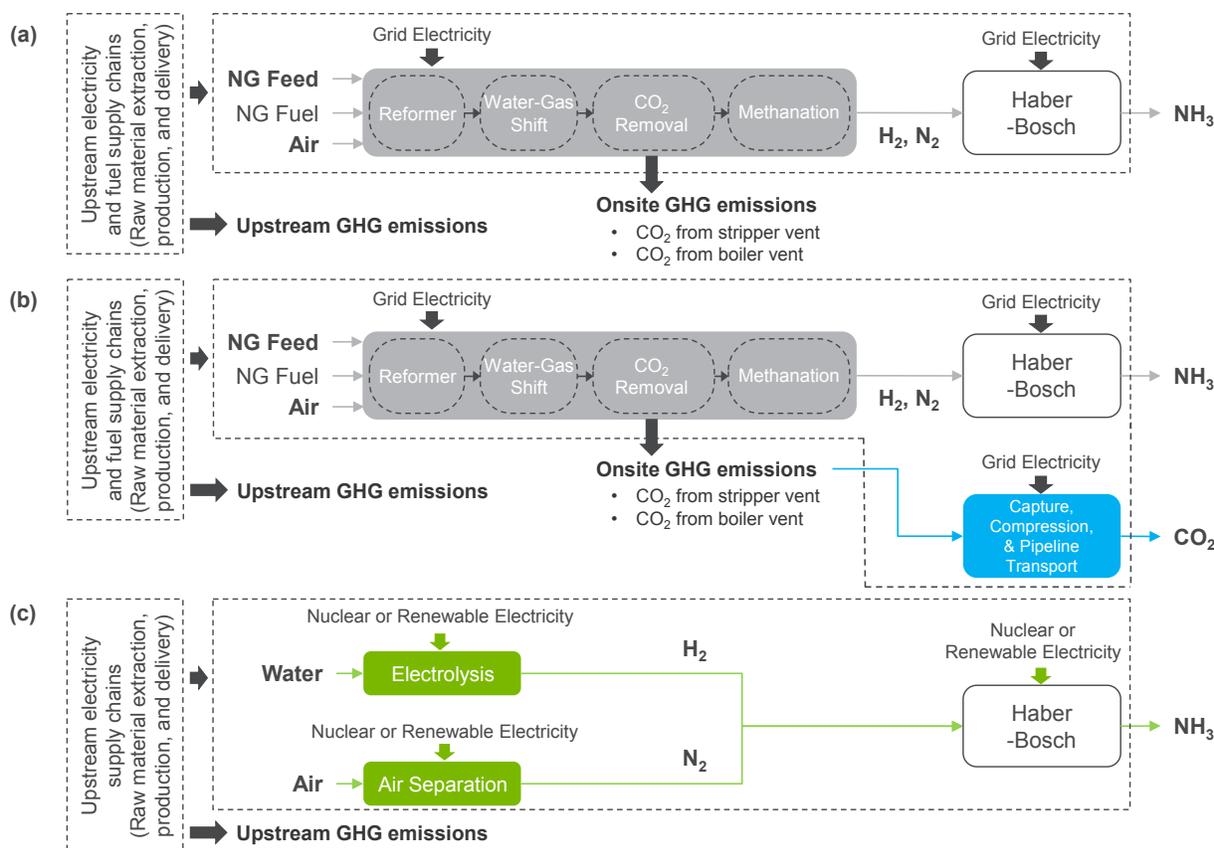
Fig. 1 System boundaries of (a) conventional NG-based ammonia production, (b) NG-based ammonia production with carbon capture, and (c) nuclear- or renewable- powered ammonia production.

sector. In addition, ammonia as a zero-carbon energy carrier could potentially be used to decarbonize other applications, such as transportation and power generation.[13] For example, ammonia can be used as a fuel in internal combustion engines to power marine vessels, or for combustion and expansion in gas turbines to generate electric power. Japan announced in 2020 that they will introduce ammonia into coal-fired power plants to reduce carbon emissions.[7] Ammonia can also be used as a hydrogen carrier and for grid storage, not only because of its relatively high volumetric energy density but also because its storage and transportation are more cost-effective compared to hydrogen storage and delivery.[8] To lower the carbon intensity of these applications, the production of ammonia needs to be carbon-free.

Most of the previous studies on techno-economic performances and life cycle impacts of various ammonia production pathways did not compare between all the conventional, carbon-capturing, and renewable ammonia production by developing each engineering process model.[3,8–11] Also, there is a lack of studies that compare the performances of various ammonia production in the United States. Liu et al. conducted the life cycle analysis (LCA) of various ammonia production options, including conventional and renewable ammonia to evaluate associated energy and carbon intensity in the United States.[7] They identified that renewable ammonia production employing renewable and carbon-free resources can reduce carbon

intensity significantly compared to conventional fossil-based ammonia production.

In this work, we develop detailed engineering process models of conventional NG-based, carbon-capturing, nuclear-powered, and renewable ammonia production using Aspen Plus®, and we expand the scope of analysis to include techno-economic analysis (TEA). NG-based ammonia is produced by the steam reforming of NG and the HB process. For the carbon-capturing ammonia option, CO_2 emitted from the steam reforming and combustion boiler is captured, pressurized, and transported via pipelines. Nuclear-powered or renewable ammonia is produced via the HB process from carbon-free hydrogen and nitrogen feedstock. In the nuclear-powered or renewable ammonia production, hydrogen is obtained from water split through electrolysis using nuclear or renewable electricity, respectively, and nitrogen is obtained via cryogenic air separation.

We conduct the TEA and LCA of these ammonia production options to calculate the levelized cost of ammonia (LCOA) production, and the associated well-to-plant-gate (WTG) GHG emissions. The cost of avoided CO_2 emissions for carbon-capturing, nuclear-powered, and renewable ammonia production is also evaluated.
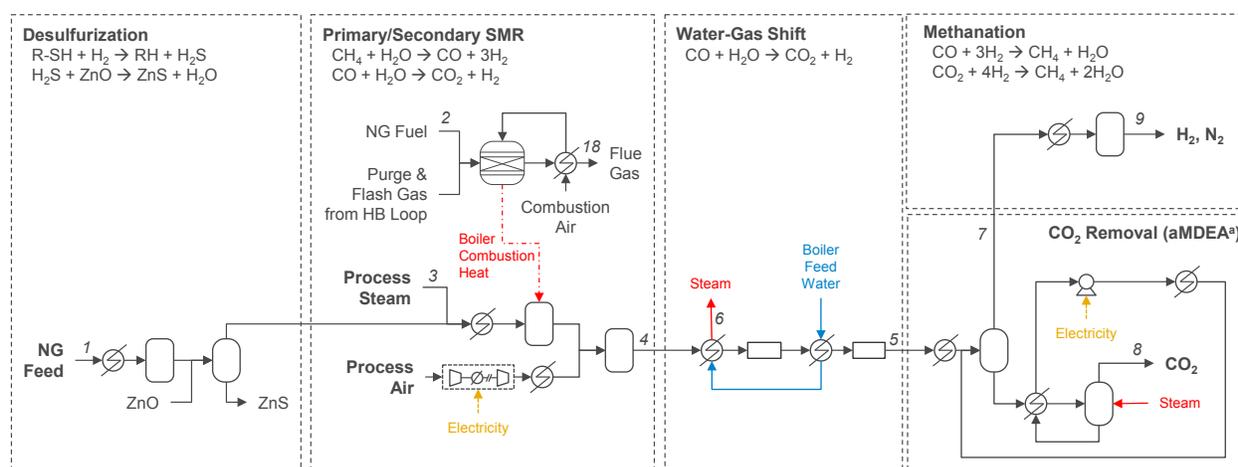
Fig. 2 Hydrogen and nitrogen production through steam reforming of NG for NG-based ammonia production.[14] Stream IDs are shown in italics. ([a] aMDEA represents activated methyl diethanolamine.)

Descriptions of ammonia production pathways and analysis methods

We developed detailed engineering process models of NG-based, carbon-capturing, and nuclear-powered or renewable ammonia production using Aspen Plus®. Fig. 1 shows schematic diagram and system boundary of each production option. In this section, each model is described in detail. Also, assumptions for TEA and LCA are described.

NG-based ammonia production

NG-based ammonia refers to the conventional HB ammonia synthesis with hydrogen produced via SMR processes. Nitrogen feedstock, sourced from the air, is concentrated by depleting oxygen via partial NG combustion in the SMR processes. The engineering process model of NG-based ammonia production was developed based on the existing model provided in the Aspen Plus example library.[14] Fig. 2 is a process flow diagram of NG-based ammonia production, and the process block is described briefly below.

Desulfurization of NG. To avoid poisoning the nickel-based catalysts used for the SMR processes, any sulfur compounds in the NG feedstock need to be removed. The pipeline NG contains 0.15–6 ppm by weight of sulfur content.[15] As shown in Fig. 2, the dry NG from the pipeline is first heated to 350°C using heat from boiler flue gas. Then NG is desulfurized in two steps using a zinc oxide (ZnO) adsorbent:[16]

$$\text{Hydrodesulfurization: R–SH + H}_2 \rightarrow \text{RH + H}_2\text{S} \qquad (1)$$
$$\text{Adsorption of H}_2\text{S by ZnO: H}_2\text{S + ZnO} \rightarrow \text{ZnS + H}_2\text{O} \qquad (2)$$
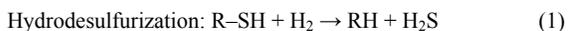
The symbol R denotes a hydrocarbon side chain. The ZnO adsorbent was assumed to be replaced every 3 years.

Steam reforming of NG. As shown in Fig. 2, the desulfurized NG is mixed with process steam, and the mixture is heated to 500°C using heat from boiler flue gas. Then the mixture is fed into the SMR section, which consists of multiple parts: pre-reformer, primary reformer, and secondary reformer.[17] In the pre-reformer, any

hydrocarbons with longer chain than methane, such as ethane, propane, and butane, etc., are rapidly converted to methane (not shown in Fig. 2). Then methane is converted to CO, CO_2, and H_2 at 31 bar in the primary SMR reactor as shown below:

$$\text{CH}_4 + \text{H}_2\text{O} \rightarrow \text{CO} + 3\text{H}_2 \qquad (3)$$
$$\text{CO} + \text{H}_2\text{O} \rightarrow \text{CO}_2 + \text{H}_2 \qquad (4)$$
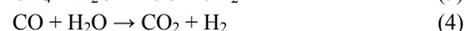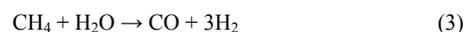
The former is the endothermic steam reforming reaction while the latter is the exothermic water-gas shift (WGS) reaction. The overall reaction in the primary reformer is endothermic; therefore, heat generated via fuel combustion needs to be provided to the SMR reactor. Details of the reaction kinetics are available in reference.[14] For conventional ammonia production, purge and flash gases from the HB loop contain unreacted hydrogen. This is combusted in the boiler to provide the heat needed for the primary reformer. Because the heat from the purge and flash gas combustion is not sufficient for the reformer, additional NG fuel is combusted in the boiler. The outlet temperature from the primary reformer is approximately 790°C.

The outlet stream from the primary reformer contains 6.3 mol% of methane. For further NG conversion, the primary reformer outlet stream is fed into the secondary reformer unit together with hot process air, which is preheated to 460°C using heat from boiler flue gas. In the secondary reformer at 31 bar, the remaining NG is partially combusted with oxygen in the air and is converted to CO, CO_2, and H_2. The partial combustion leads to more hydrogen production, concentrates N_2 from the air by depleting O_2, and generates heat to sustain the conversion process. The outlet temperature from the secondary reformer is approximately 980°C. The outlet stream includes 35.5 mol% of H_2, 35.3 mol% of H_2O, 15.2 mol% of N_2, 8.4 mol% of CO, 5.1 mol% of CO_2, 0.4 mol% of CH_4, and 0.2 mol% of Ar. The flow rate of process air is controlled so that the H_2/N_2 ratio in the stream entering the HB loop is close to 3.

WGS reactions. The outlet stream from the secondary reformer is cooled to 380°C using boiler feedwater, then the stream is fed into two series of WGS reactors. The high-temperature shift (HTS) reaction occurs with the presence of high-temperature catalysts (iron-
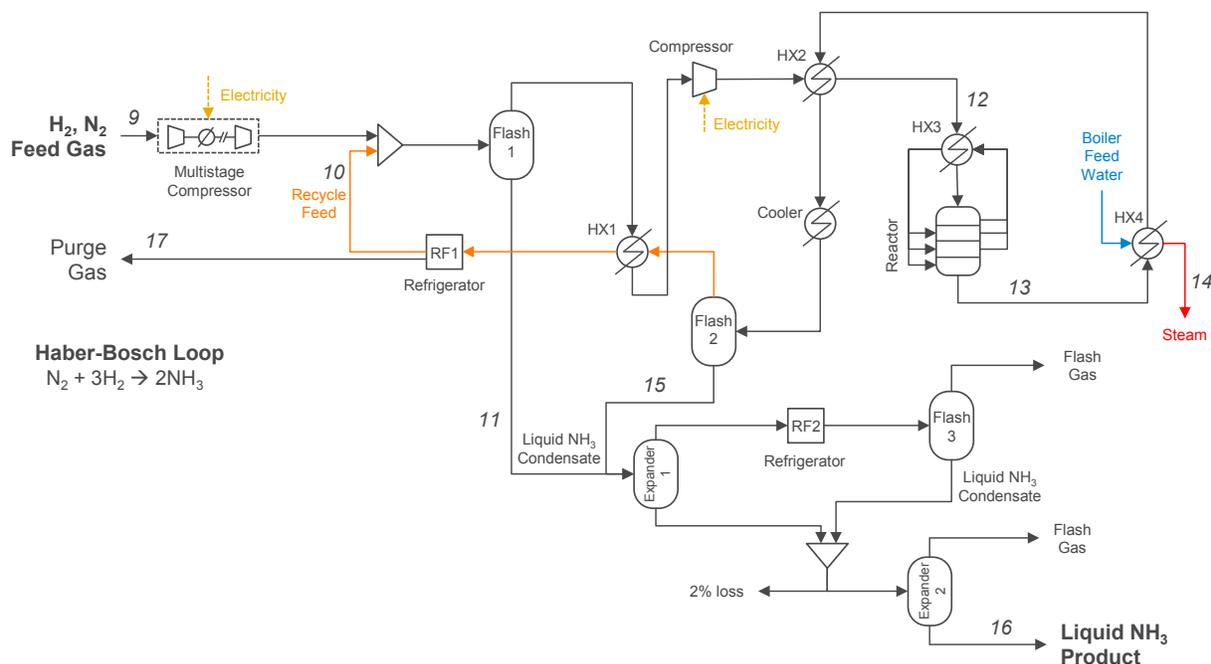
Fig. 3 HB loop for ammonia production.[14] Stream IDs are shown in italics.

chromium) and is followed by a low-temperature shift (LTS) reaction to improve the overall hydrogen production yield.[18] The WGS reaction is as follows:

$$CO + H_2O \rightarrow CO_2 + H_2 \qquad (5)$$
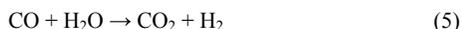
The HTS reactor converts CO and the remaining H_2O into CO_2 and H_2 at 29 bar.[14] The outlet stream from the HTS reactor still contains 2.2 mol% of CO. The WGS reaction is exothermic, so the temperature of the outlet stream from the reactor rises to 450°C. This is cooled to 210°C using boiler feedwater, and then is fed into the LTS reactor at 28 bar for the conversion of the remaining CO.[14] The details for the WGS reaction kinetics are available in reference.[14] The outlet stream from the LTS reactor includes 43.6 mol% of H_2, 27.2 mol% of H_2O, 15.2 mol% of N_2, 13.2 mol% of CO_2, 0.4 mol% of CH_4, 0.2 mol% of CO, and 0.2 mol% of Ar. In addition, high-quality steam at 408°C and 112 bar is generated from this section by heating boiler feedwater to cool down the H_2/N_2 stream across the WGS reactors. This steam is used to generate electricity that is consumed onsite for compressor and pump units.

CO_2 removal by aMDEA process. The WGS outstream contains HB reaction feedstocks of both H_2 and N_2, as well as impurities, such as CO_2. The large amount of CO_2 is often removed by amine-based solvent capture. Traditionally, methyl ethanolamine (MEA)-based CO_2 capture technology was used for conventional ammonia production.[19] In addition, many existing TEA papers that analyzed conventional ammonia production assumed MEA-based technology.[3,9] However, aMDEA (activated methyl diethanolamine)-based capture technology has recently become popular for ammonia production, because it requires less energy and does not lose any of the active solvent components.[16] Moreover, its CO_2 removal rate is

higher than that of traditional MEA-based technology.[20,21] Since it is difficult to achieve a high CO_2 removal rate solely by using an MDEA solvent, an activator such as piperazine (PZ) is used together with MDEA to enhance the CO_2 removal rates. In this work, PZ/MDEA-based CO_2 capture technology was assumed for NG-based ammonia production.

The H_2/N_2 stream is cooled to 40°C using cooling water, and then more than 99% of CO_2 is removed from the H_2/N_2 stream by an absorber unit at 26.5 bar. The CO_2-rich PZ/MDEA solvent from the absorber is regenerated by heating. It is heated to approximately 110°C using a heat exchanger while cooling the hot lean solvent from a stripper unit. The PZ/MDEA solvent is regenerated at 130°C from the striper by removing CO_2. The removed CO_2 gas contains 97 mol% of CO_2. In NG-based ammonia production, this corresponds to process CO_2 emissions. The regenerated lean solvent is pressurized to 26.5 bar, cooled to 50°C, and fed into the absorber. The aMDEA capture technology shows no losses of the active solvent components due to their low vapor pressures.[16] Therefore, we assumed no replacement of PZ/MDEA during the plant lifetime.

Methanation of oxygen-containing molecules. The treated gas from the aMDEA process still contains 0.4 mol% of CO and a tiny amount of CO_2, which can lead to the deactivation of the iron-based HB catalysts due to oxidation. To prevent catalyst deactivation, the treated H_2/N_2 stream is heated to 280°C, and then CO and CO_2 are converted to CH_4 by methanation reactions at 26.5 bar as follows:

$$CO + 3H_2 \rightarrow CH_4 + H_2O \qquad (6)$$
$$CO_2 + 4H_2 \rightarrow CH_4 + 2H_2O \qquad (7)$$
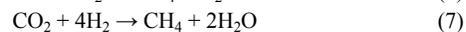
The details in the reaction kinetics are available in reference.[14] The resulting gas stream contains 74.8 mol% of H_2, 24.9 mol% of N_2, and
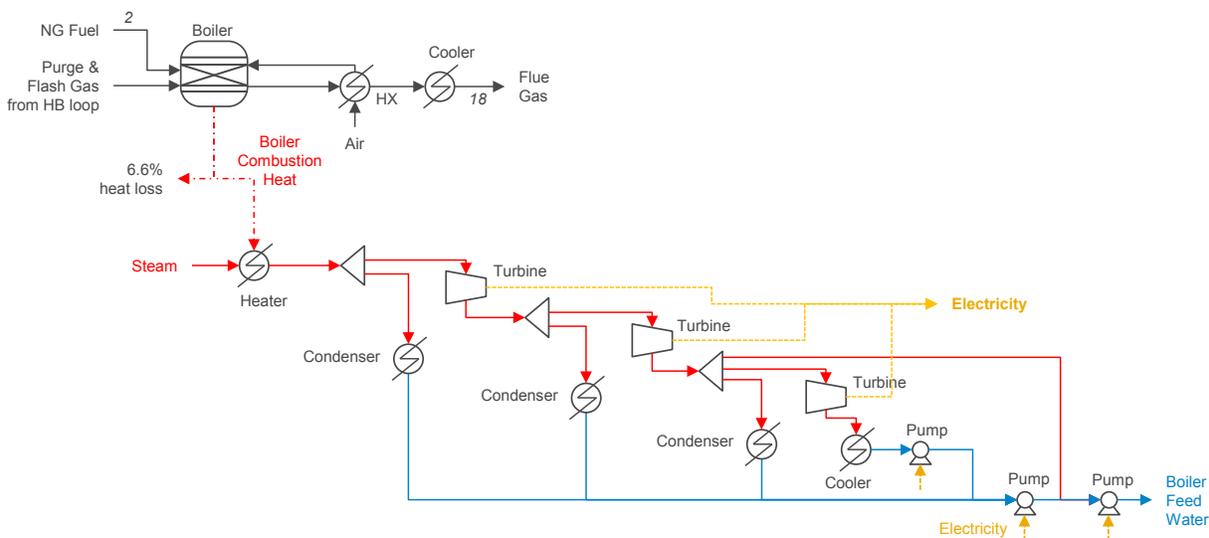
Fig. 4 Boiler and steam turbine systems.[22] Stream IDs are shown in italics.

0.4 mol% of CH_4. In contrast to CO_2, the CH_4 is inactive in the HB process. The H_2/N_2 ratio is approximately 3.

HB loop. Fig. 3 shows a process flow diagram of the HB loop in this work. The feed gas stream goes through a multistage compressor with intercooling and leaves the compressor at 30°C and 275 bar. This compressor uses a large amount of electricity. The feed gas leaving the compressor is then mixed with the recycle stream from the HB loop. The liquid phase accounts for 3.5 mol% of the mixture, composed of the make-up and recycle streams. The liquid phase is separated from the mixture in a gas–liquid separator (Flash 1) with an NH_3 purity of 98.3 mol%. The remaining gas stream from the separator is heated to 28°C in a heat exchanger (HX1) and compressed to 292 bar, which is the operating pressure of an ammonia synthesis reactor. The gas stream is further heated in heat exchangers (HX2 and HX3) and enters the HB reactor. The reactor inlet stream consists of 70 mol% of H_2, 23 mol% of N_2, 3 mol% of CH_4, and 5 mol% of NH_3. The oxygen content in the inlet stream is less than 1 ppm, which is smaller than the maximum allowable oxygen impurity level for ammonia synthesis (3 ppm).[16]

The HB ammonia synthesis reactor was modeled by four plug flow reactors. The details in the reaction kinetics are available in reference [14]. In this work, nitrogen and hydrogen react at 284–292 bar and 300–500°C to synthesize ammonia. The product gas exiting the HB reactor consists of 54 mol% of unreacted H_2, 17 mol% of unreacted N_2, 3 mol% of CH_4, and 25 mol% of NH_3. The ammonia conversion yield from nitrogen per pass through the synthesis loop is 35 mol%, which is in the range of typical conversion yield (25–35 mol%).[16] The low conversion ratio is due to thermodynamic equilibrium limitations of the ammonia synthesis reaction.[9]

The excess heat in the product stream can be used to generate steam. In this work, the product stream is cooled in a heat exchanger (HX4) by exchanging heat with high-pressure boiler feedwater to generate steam. The steam can be used in the turbine to generate electricity to compensate for the work needed by the compressors. The

remaining heat in the product stream is used in a heat exchanger (HX2) to heat the gas mixture entering the HB reactor.

The product stream is further cooled to 45°C. The cooled stream contains 15.9 mol% of the liquid phase, which is separated in a gas–liquid separator (Flash 2). The condensed liquid stream has an NH_3 purity of 97 mol%. The gaseous portion in the separator contains mainly unreacted gas. It is cooled down to 36°C in a heat exchanger (HX1) by the incoming stream to the HB loop and sent to the first refrigeration section (RF1). This work considered an ammonia refrigeration loop. In the refrigerator, a depressurized ammonia refrigerant is evaporated to cool the process stream. The vaporized refrigerant is regenerated through compression and cooling.[3] A small portion (3%) of the gaseous stream is then purged out of the HB loop to prevent the buildup of inert gas (i.e., argon) in the loop. The purge gas can be combusted in a boiler to generate heat. The remaining flow is mixed with the make-up gas stream, where the loop starts from the beginning again.

Liquid NH_3 condensed from gas–liquid separators (Flash 1 and 2) is expanded to 30 bar in expander 1. The gaseous portion after the expander is sent to a second refrigeration section (RF2) to condense additional ammonia. Then additional liquid ammonia condensate can be obtained from a gas–liquid separator (Flash 3). The mixed liquid ammonia stream is expanded to 20 bar in Expander 2 to store liquid ammonia. The liquid ammonia from the expander is the final product, with an NH_3 purity of 99.9 mol%. In the entire HB synthesis loop, 89 mol% of nitrogen is converted to ammonia. In this work, 1,270 MT of ammonia is produced using 870 MT of NG each day.

The excess heat in the product stream can be used to produce steam. The purge and flash gases from the HB loop can be combusted in a boiler to raise the temperature of steam,[16] which can then be used in the turbine to generate electricity to compensate for the work needed by the compressors in the HB system. These gases consist of 58 mol% of H_2, 19 mol% of N_2, 5 mol% of CH_4, and 19 mol% of NH_3. To avoid NO_x gas emissions from the combustion boiler, 95% of NH_3
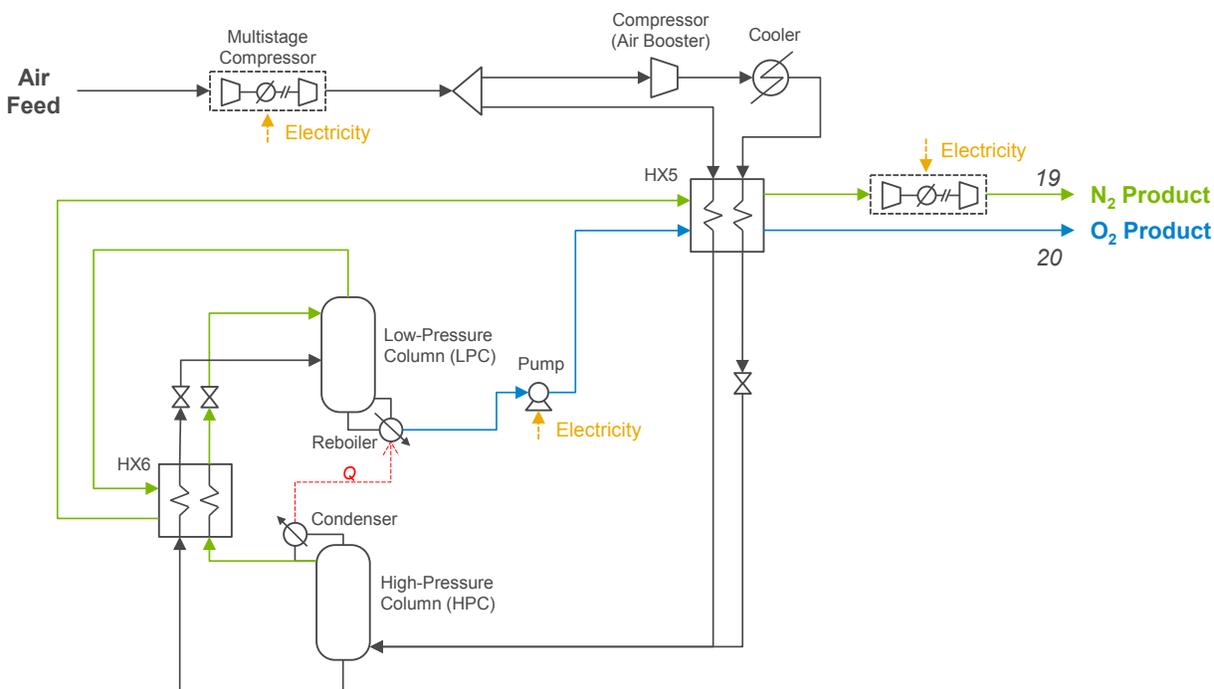
Fig. 5 Nitrogen production via cryogenic air separation.[35] Stream IDs are shown in italics.

gases were assumed to be removed from flash and purge gases by water scrubbing before entering the boiler (not shown in Fig. 3).[14,16]

Steam turbines and utility. In this work, we employed the existing engineering model for the boiler and steam turbine systems.[22] Fig. 4 is a process flow diagram of boiler and steam turbine systems. Steam generated from the WGS and HB sections is used to produce electricity, which is consumed onsite for compressors and pumps. The net electricity requirement is still positive; therefore, grid electricity needs to be used to supply power for NG-based ammonia production. Then steam is condensed and pumped to regenerate the high-pressure boiler feedwater. Any steam needed for NG-based ammonia production (e.g., process steam for SMR) is provided by separating steam after a medium-pressure turbine (not shown in Fig. 4). In addition, the existing engineering model for cooling tower systems was employed.[23,24] In this work, 0.15% of cooling water was assumed to be provided as make-up cooling water.

Carbon-capturing ammonia production

As described previously, carbon-capturing ammonia refers to the ammonia produced from fossil resources. This is the same as NG-based ammonia. However, for carbon-capturing ammonia, onsite CO_2 emissions from ammonia production are captured to be sequestrated or used for other applications to reduce carbon intensity.

In this work, we considered two versions of the carbon-capturing ammonia production design. One is to capture only process CO_2 emission that has higher CO_2 concentration thus lower capture cost by the aMDEA process. We call this carbon-capturing ammonia version 1. The second (version 2) is to capture both process and combustion CO_2 emissions, which would increase capture cost by enabling a greater degree of CO_2 reduction. The combustion emissions

correspond to the boiler flue gas emissions as shown in Fig. 4. For carbon-capturing ammonia version 2, the combustion emissions are captured by Shell's Cansolv process, which employs an amine-based solvent.[25,26]

Carbon-capturing ammonia version 1: Capturing process CO_2 emissions. For NG-based ammonia production, the aMDEA process removes a substantial amount of CO_2 from the H_2/N_2 stream. For carbon-capturing ammonia version 1, this captured CO_2 is further purified to meet CO_2 pipeline specifications. The water content is reduced below 600 ppm by weight using Joule-Thomson cooling systems (to avoid the corrosion of CO_2 pipelines).[27–29] Then, to transport it via CO_2 pipelines, it is pressurized to 2,200 psig and cooled to approximately 50°C.[30] Additional energy consumption and costs for the compression and transportation of CO_2 were considered when investigating techno-economic performances and life cycle impacts of this carbon-capturing ammonia option. In addition, another cooling tower system for the cooling of CO_2 is installed for carbon-capturing ammonia production by assuming the existing NG-based ammonia production system does not have the remaining cooling capacity.[30]

Carbon-capturing ammonia version 2: Capturing process and combustion CO_2 emissions. In this case, all onsite CO_2 emissions from NG-based ammonia production are captured. Process CO_2 emissions are captured by the aMDEA process. In addition, 90% of the boiler combustion CO_2 emissions are captured by Cansolv process.[25,26] The captured CO_2 goes through the same treatments to be transported via CO_2 pipelines as described in the previous section. Additional steam is required for the Cansolv process.

CO_2 pipeline transportation. For both carbon-capturing ammonia versions, the captured CO_2 is transported to consumers via

CO_2 pipelines. In this work, we employed the National Energy Technology Laboratory (NETL)'s CO_2 transport cost model to analyze cost and energy associated with CO_2 pipeline transportation.[31] Sensitivity analyses were performed for pipeline transport distances from 100 to 1,000 miles by employing 500 miles as the baseline distance.

Nuclear-powered or renewable ammonia production

Nuclear-powered or renewable ammonia refers to ammonia production from carbon-free sources using nuclear or renewable power, respectively, instead of using fossil resources and grid electricity. In this work, we considered clean hydrogen production via water electrolysis using nuclear or renewable power and nitrogen production via cryogenic air separation. Nuclear-powered or renewable ammonia is then synthesized through the HB loop. In this work, nuclear or renewable electricity was assumed to power cryogenic air separation and the HB loop for nuclear-powered or renewable ammonia production, respectively.

Clean hydrogen production via electrolysis. In this work, we employed the existing TEA results for clean hydrogen production via water electrolysis.[32,33] The stoichiometric amount of hydrogen with a purity of 100% was assumed to be provided to the HB loop. Two types of clean hydrogen production were considered: (1) the state-of-the-art (SOA) low-temperature electrolysis (LTE) using polymer electrolyte membrane,[32] and (2) the SOA high-temperature electrolysis (HTE) using solid oxide electrolyzer.[33]

In addition, we assumed that carbon-free energy sources are used to provide the energy needed for water electrolysis. Renewable electricity such as wind and solar power was assumed for LTE, while nuclear power was considered for HTE.

Nitrogen production via cryogenic air separation. For the nuclear-power or renewable ammonia production options, nitrogen is prepared by air separation. Nitrogen can be separated from air by membrane permeation, pressure swing adsorption, or cryogenic distillation. Because the oxygen impurity level should be less than 10 ppm to avoid catalyst poisoning for ammonia synthesis, permeation is not an appropriate technology for air separation in this case. In addition, because a typical ammonia production plant capacity is 1,200–3,000 MT/day, cryogenic distillation is the most suitable air separation technology not only because the typical capacity of cryogenic distillation is large enough for ammonia production, but also because it is the most widely used, mature technology for high-purity nitrogen production by air separation.[34]

The engineering model of nitrogen production by cryogenic distillation was developed using Aspen Plus® based on the existing engineering modeling work from the literature.[35] Cryogenic distillation produces high-purity nitrogen and oxygen streams. Fig. 5 is a process flow diagram of nitrogen production via cryogenic air separation. The dry air feed (78% N_2, 21% O_2, and 1% Ar) is compressed to a pressure of 6.6 bar and split into two streams. One stream (68% of the air feed) is cooled in a heat exchanger (HX5) to cryogenic temperatures while heating N_2 and O_2 product streams. The other stream is further compressed in an air booster to 12 bar, sent to the heat exchangers, and then expanded to 6.6 bar to lower its temperature.

Both streams are fed into the bottom of the high-pressure cryogenic distillation column (HPC) with 45 theoretical separation stages at a pressure between 5.1 and 6.6 bar. The O_2-enriched liquid stream is obtained at the bottom of HPC. In addition, a total condenser is used in HPC to collect high-purity liquid nitrogen at the top. By setting the oxygen impurity level of the nitrogen stream to 1 ppm,[34] HPC separates 42.2% of the nitrogen in the air.

Both top and bottom streams from the HPC are cooled in a heat exchanger (HX6), expanded to 1.3 bar, and then fed into a low-pressure cryogenic distillation column (LPC) with 100 theoretical stages. LPC is operated at 1.3 bar. A kettle-type reboiler is used in the LPC to collect high-purity liquid oxygen at the bottom. The nitrogen stream from HPC is also provided as reflux to the top of the LPC. The oxygen impurity level of the nitrogen product stream at the top is set to 10 ppm, which is the maximum oxygen impurity level tolerable to avoid catalyst poisoning for ammonia synthesis.[16] LPC produces high-purity nitrogen and oxygen streams with purities of more than 99.99 mol% including argon.

The heat required by the reboiler in LPC can be obtained from the condenser in HPC. Thus, in practice, the LPC is installed on top of the HPC to form a combined reboiler/condenser heat transfer unit. A temperature difference of 1–2 degrees between the reboiler and condenser should be maintained to enable proper heat transfer.[34] The total heat duty of the unit is set to zero.

The nitrogen product stream from the LPC enters a heat exchanger (HX6) to cool the input streams to the operation temperature of the LPC. Then it is fed into a heat exchanger (HX5) to cool the pressurized air feed streams. The liquid oxygen product stream from the LPC is pressurized to 4.7 bar and flashed in the heat exchanger (HX5) to cool the feed streams. Last, the nitrogen product stream is compressed to 20 bar and employed as a feed gas for ammonia synthesis. The resulting nitrogen and oxygen streams have purities of 97.2 mol% and 100 mol%, respectively, excluding argon. The nitrogen purity level including argon is more than 99.99 mol%.

HB loop and steam turbines. The nitrogen stream from cryogenic air separation is compressed to 20 bar and mixed with pure hydrogen at 20 bar, which is obtained through water electrolysis. Subsequently, the mixed stream is compressed to 275 bar, then is introduced into the HB ammonia synthesis loop shown in Fig. 3. For the comparison of nuclear-powered or renewable ammonia production with NG-based ammonia production, we specified that the nitrogen and hydrogen flow rates in the make-up gas feed stream are the same for both engineering models. We also adjusted the cooling capacity of a cooler and RF1 in Fig. 3 so that we have the same liquid NH_3 condensate flow rates from gas–liquid separators (Flash 1 and 2 in Fig. 3) for both NG-based and nuclear-powered/renewable ammonia production models. The nuclear-powered or renewable ammonia systems do not emit carbon-based GHG components, such as CO_2 and CH_4, during the operation because they do not use any carbon material in the systems.

The boiler and steam turbine systems shown in Fig. 4 were employed for nuclear-powered or renewable ammonia production. In case of NG-based ammonia production, additional NG fuel (stream ID 2 in Fig. 4) is combusted in a boiler to provide sufficient heat to the steam reformer. Therefore, the nuclear-powered or renewable ammonia production options do not need to employ additional NG fuel for the boiler and steam turbine systems. Only purge and flash

gases from the HB loop are combusted in a boiler to raise the temperature of steam, which is produced by using the excess heat in the product stream from the HB loop. The steam is then used in the turbine to generate electricity, which is consumed onsite by compressors in the HB system.

TEA of ammonia production

TEA of ammonia production was performed using the H2A (Hydrogen Analysis) Production Model version 3.2018.[36] All the dollar values in this paper were based on 2016 U.S. dollars. The LCOA was calculated to obtain a zero net present value with 8% of the internal rate of return over an operating period of 40 years. A 90% capacity factor was assumed for ammonia production. The rest of the assumptions for TEA are listed in Table S1 of the Supplementary Information.

Equipment and installation costs for all processes (except for the Cansolv process) were determined from mass and energy balance results obtained from engineering models using Aspen Process Economic Analyzer. The costs for the Cansolv process were obtained from reference [26] and scaled based on the CO_2 flow rate. Labor costs were estimated based on the number of equipment units in engineering models, using an approach described in reference.[23,37] The amount of feedstock, catalysts, and energy needed was calculated from mass and energy balance results obtained from engineering models. The information about the lifetime and price of catalysts in this work was obtained from the literature.[9]

In this work, CO_2 transportation costs[31] and carbon capture tax credits[38] were added to the LCOA of carbon-capturing ammonia production. The tax credit amount was determined by the Section 45Q tax credit for carbon capture projects.[38] Depending on the use of captured CO_2, $35 to $50 of CO_2 tax credits can be claimed per 1 MT of CO_2 capture. Details of the costs of equipment, feedstock, utility, byproduct, catalysts, and CO_2 pipeline transportation used in this work are available in Sections S2–S4 of the Supplementary Information.

The following four clean hydrogen production costs were considered for TEA of nuclear-powered and renewable ammonia production in this work:

1. $4.83/kg H_2: Cost of clean H_2 using SOA LTE.[32]
2. $4.16/kg H_2: Cost of clean H_2 using SOA HTE.[33]
3. $2.00/kg H_2: DOE 2020 target cost of clean H_2.[39]
4. $1.00/kg H_2: Long-term target cost of clean H_2 that can be cheaper than that of conventional SMR-based H_2.[40]

The existing TEA models of SOA LTE and SOA HTE calculated the current clean hydrogen production cost to be $4.83/kg H_2 and $4.16/kg H_2, respectively, when assuming $0.07/kWh of electricity price for electrolysis.[32,33] According to the reference,[32] the cost of clean H_2 using SOA LTE could be decreased to $2.31/kg H_2 when a cheaper electricity cost of $0.03/kWh is assumed. On the other hand, the H_2 production cost using SOA LTE could be increased to $6.99/kg H_2, which corresponds to the upper end of the expected cost spread determined by Monte Carlo multi-variable analysis. Similarly, the cost of clean H_2 using SOA HTE could vary from $2.36 to $5.71/kg H_2.[33]

Given that the current SMR-based H_2 cost is much cheaper ($1.15/kg H_2), clean H_2 production cost needs to be lower to be competitive with the market ammonia product. According to the U.S. Department of Energy (DOE),[39] the 2020 target clean H_2 levelized cost was $2.00/kg H_2. This target cost could be achieved with electrolysis technologies for clean H_2 production if capital costs are decreased and net system energy efficiency and stack service lifetime are increased. According to Peterson et al.,[32,33] $1.86 and $2.00 per kg H_2 of production costs were estimated for clean H_2 produced assuming $230/kW and $360/kW for LTE and HTE, respectively, and $0.03/kWh for electricity price.

More recently, the DOE's Hydrogen Energy Earthshots Initiative with a goal to reduce the clean H_2 production cost to $1 per 1 kg H_2 within 1 decade (1-1-1), representing approximately 80% reduction from current production costs.[40] This cost is lower than $1.15/kg H_2 of the current SMR-based H_2 production cost.

For nuclear-powered or renewable ammonia production, high-purity oxygen is also produced as a byproduct from cryogenic air separation, as shown in Fig. 5. Byproduct credits for oxygen were considered for the TEA of those ammonia production options. In addition, energy price data were updated using the recent Energy Information Administration's Annual Energy Outlook (AEO) data for 2021.[41] According to the AEO data for 2021, industrial electricity and industrial NG prices were $0.07/kWh and $4.24/MMBtu–LHV (low heating value), respectively, which were slightly cheaper than those reported from the previous AEO data in 2017.

LCA of ammonia production

For the modeled ammonia facility, the onsite GHG emissions data were estimated based on the mass and energy balance results from the engineering models. As shown in Fig. 1 and described previously, NG-based ammonia production has two major GHG emission sources, one is process CO_2 emissions from the aMDEA process, and the other is combustion CO_2 emissions in flue gas from the boiler. Carbon-capturing ammonia production compresses and transports the captured CO_2 emissions. On the other hand, nuclear-powered and renewable ammonia production pathways do not have any onsite GHG emissions because they do not use any carbon feedstock. GREET (Greenhouse gases, Regulated Emissions, and Energy use in Technologies) model data were used to account for upstream GHG emissions associated with the upstream activities of grid electricity generation and NG supply for ammonia production.[42] WTG GHG emissions of ammonia production refer to the combined onsite and energy supply chain GHG emissions.

In this work, indirect GHG emissions associated with the manufacture of equipment and associated construction materials, such as solar panels and wind turbines, are not accounted for. Quantifying the impacts of equipment embodied emissions is being currently investigated and will be reported in future publications. The impacts of embodied emissions in solar photovoltaic and wind turbine on the renewable ammonia carbon intensity will likely be significant.

For nuclear-powered/renewable ammonia production, oxygen is generated as a byproduct. Mass-based allocation was performed to allocate energy use and emissions associated with air feed compressors between oxygen and nitrogen products from cryogenic air separation. Electricity generated from the steam turbines is also

consumed onsite for compressor and pump units. The generated electricity was allocated between those units to account for energy consumption for each modeling block (for example, HB block and SMR block).

CO$_2$ avoidance cost calculation

In this work, alternative ammonia production options, such as carbon-capturing, nuclear-powered, and renewable ammonia production, aim to reduce the carbon intensity of ammonia production. For those alternative options to be cost-competitive to conventional NG-based ammonia, the costs of avoided CO$_2$ emissions for carbon-capturing, nuclear-powered, and renewable ammonia production were calculated using the following equation:

$$\text{CO}_2 \text{ avoidance costs} = \frac{\Delta(\text{LCOA of alternative and conventional production})}{\Delta(\text{WTG GHG emissions of conventional and alternative production})} \quad (8)$$

The lower CO$_2$ avoidance cost indicates that the lesser CO$_2$ tax benefit is needed for alternative production to be cost-competitive to conventional production.

Results and discussion

Process modeling results

Physical values for streams in the NG-based and nuclear-powered/renewable ammonia production systems are shown in Table S2 of the Supplementary Information. Different compositions in the make-up feed gas (e.g., CH$_4$ content in the conventional system) result in different flash temperature conditions to collect the same NH$_3$ condensate flow rates between both systems.

Table 1 provides details about energy consumption and generation for the production of NG-based, carbon-capturing, and nuclear-powered/renewable ammonia. While the nuclear-powered or renewable ammonia options do not use any NG, the conventional NG-based option employs NG as a process gas and fuel to produce hydrogen in the SMR process. A total of 32.5 GJ NG per MT NH$_3$ is used for the conventional system. This is similar to the result in our previous study.[7]

For nuclear-powered or renewable ammonia production, 0.62 GJ electricity is required for producing one MT N$_2$ at 20 bar. This is comparable to the result in our previous study[7]. Also, the HB loop in this work requires 1.29 GJ electricity to produce one MT NH$_3$. One previous study[7] estimated that about 1.17 GJ electricity was needed for the HB loop. The difference can be attributed to the different operating pressures assumed for the HB loop. While the previous work assumed an operating pressure of 200 bar, this work considered 292 bar[14].

Energy efficiencies for ammonia production are shown in Table 1. Energy efficiencies (η) are calculated by the following equations:

$$\eta = \frac{(\dot{m}_{NH_3} \times LHV_{NH_3})}{\dot{m}_{NG} \times LHV_{NG} + W_{Utility}} \quad (9)$$

for NG-based and carbon-capturing ammonia,

$$\eta = \frac{(\dot{m}_{NH_3} \times LHV_{NH_3})}{\dot{m}_{H_2} \times LHV_{H_2} + W_{Utility}} \quad (10)$$

for nuclear-powered and renewable ammonia, where $\dot{m}_{NH_3}$, $\dot{m}_{NG}$, and $\dot{m}_{H_2}$ refer to the mass flow rates of ammonia, NG, and hydrogen. LHV represents the low heating value, and $W_{Utility}$ corresponds to net electricity consumption. LHVs of NH$_3$, NG, and H$_2$ are 18.6 MJ/kg NH$_3$[43], 47.1 MJ/kg NG, and 120 MJ/kg H$_2$, respectively. Energy efficiencies of carbon-capturing ammonia are smaller than that of NG-based ammonia due to the increased consumption of grid electricity for CO$_2$ capture, compression, and transport. In contrast, the energy efficiency of nuclear-powered and renewable ammonia is calculated to be 77.1%, starting from H$_2$ feedstock. If we expand the system boundary of nuclear-powered/renewable ammonia production to account for the electricity consumption for clean hydrogen production via electrolysis, the energy efficiency of nuclear-powered and renewable ammonia production is decreased to the range of 46.5–55.3%, as the energy efficiency of clean hydrogen ranges from 60.1–71.4% depending on the electrolysis technology[32,33].

Table S6 of the Supplementary Information represents the carbon balance for NG-based and carbon-capturing ammonia production. All values are converted to have a unit of kmol-C/hr. Differences between system inputs (process NG, NG fuel, and air feed) and system outputs

Table 1 Energy consumption and generation for various ammonia production pathways. All values are based on the low heating value (LHV) of materials.

Production Pathways	NG-based NH$_3$	C-capturing NH$_3$ v1	C-capturing NH$_3$ v2	Nuclear-powered or renewable NH$_3$
Natural Gas (GJ/MT NH$_3$)[a]	32.52	32.52	32.52	0
Clean H$_2$ (GJ/MT NH$_3$)[a]	0	0	0	23.67
Electricity (GJ/MT NH$_3$)[a]	0.22	0.71 (±0.07)	1.23 (±0.03)	0.43
ASU[b]	0	0	0	0.51
SMR[c]	0.36	0.36	0.36	0
aMDEA[d]	0.21	0.21	0.21	0
Cansolv and CO$_2$ Compression	0	0.39	0.62	0
CO$_2$ Transport	0	0.10 (±0.07)	0.06 (±0.03)	0
HB[d]	1.18	1.18	1.18	1.29
Power Generation	1.53	1.53	1.19	1.37
Energy Efficiency, η (%)	56.7	55.9 (±0.1)	55.0 (±0.1)	77.1

[a] MT = metric tons. [b] ASU = air separation units. [c] SMR = steam methane reforming. [d] aMDEA = activated methyl diethanolamine. [e] HB = Haber-Bosch.
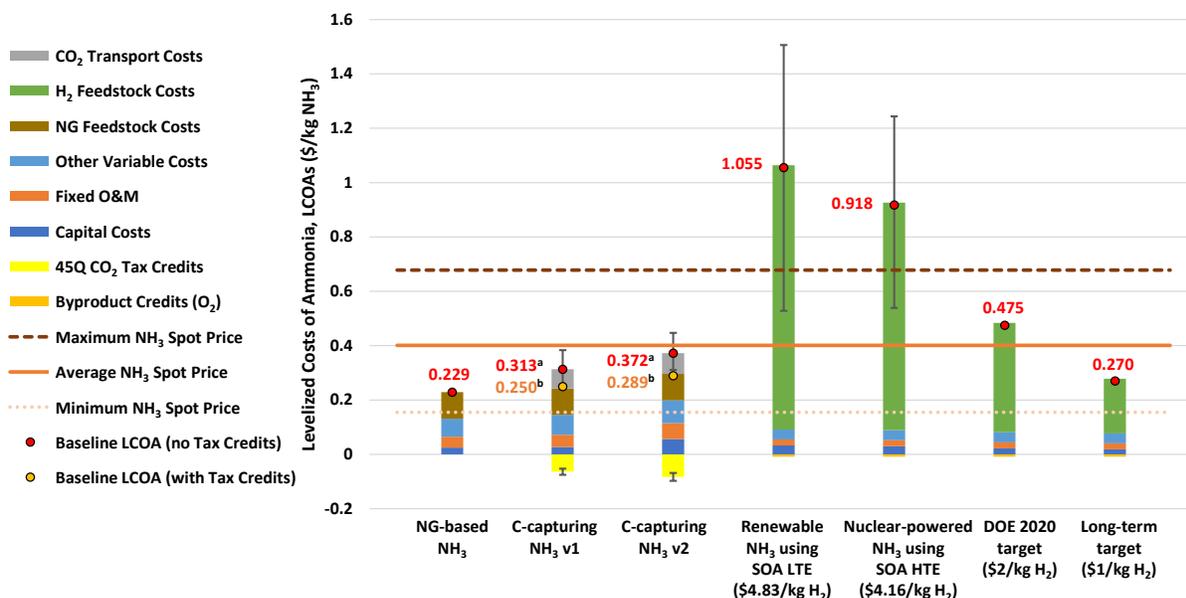
Fig. 6 Levelized costs of ammonia (LCOA) for NG-based, carbon-capturing, nuclear-powered, and renewable ammonia production. Error bars for carbon-capturing ammonia are attributed to the sensitivity analyses for 100 to 1,000 miles of CO_2 pipeline transport distances and \$35 to \$50 per MT CO_2 of carbon capture tax credits. Error bars for renewable and nuclear-powered NH_3 are attributed to the variation of clean H_2 production costs. DOE 2020 and long-term target cases represent nuclear-powered or renewable ammonia production costs using the DOE 2020 and long-term target costs of clean H_2, respectively. NH_3 spot price represents the spot price observed during 2000–2019 in U.S. Tampa.[8] ([a] LCOA of carbon-capturing ammonia without considering CO_2 tax credits. [b] LCOA of carbon-capturing ammonia with considering CO_2 tax credits.)
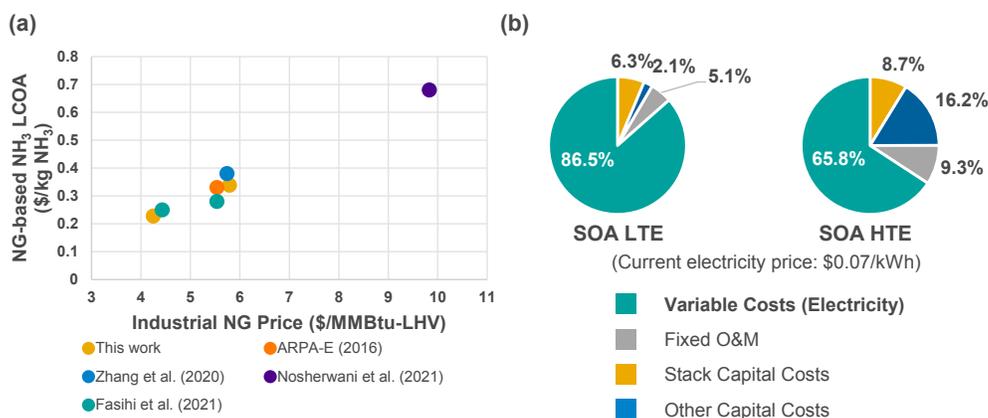
Fig. 7 (a) NG-based NH_3 LCOA from multiple studies[3,9,44,45] that employed different NG prices. (b) Breakdown of clean H_2 costs produced via the state-of-the-art low temperature electrolysis (SOA LTE)[32] and the state-of-the-art high temperature electrolysis (SOA HTE).[33]

(NH_3 product, process gas emissions, flue gas emissions, and captured CO_2) for NG-based and carbon-capturing ammonia production are negligible (0.065% differences); therefore, the production systems are closed with respect to the carbon flow. NG-based ammonia production has significant process gas and flue gas emissions. On the other hand, carbon-capturing ammonia production version 1 captures most of the process CO_2 emissions by the aMDEA process. Carbon-capturing ammonia production version 2 captures not only process

CO_2 emissions but also flue gas CO_2 emissions by the Cansolv process.

TEA results

Fig. 6 shows the LCOAs of NG-based, carbon-capturing, nuclear-powered, and renewable ammonia production. LCOA of NG-based ammonia production is calculated to be \$229 per MT of NH_3. The

Green Chemistry
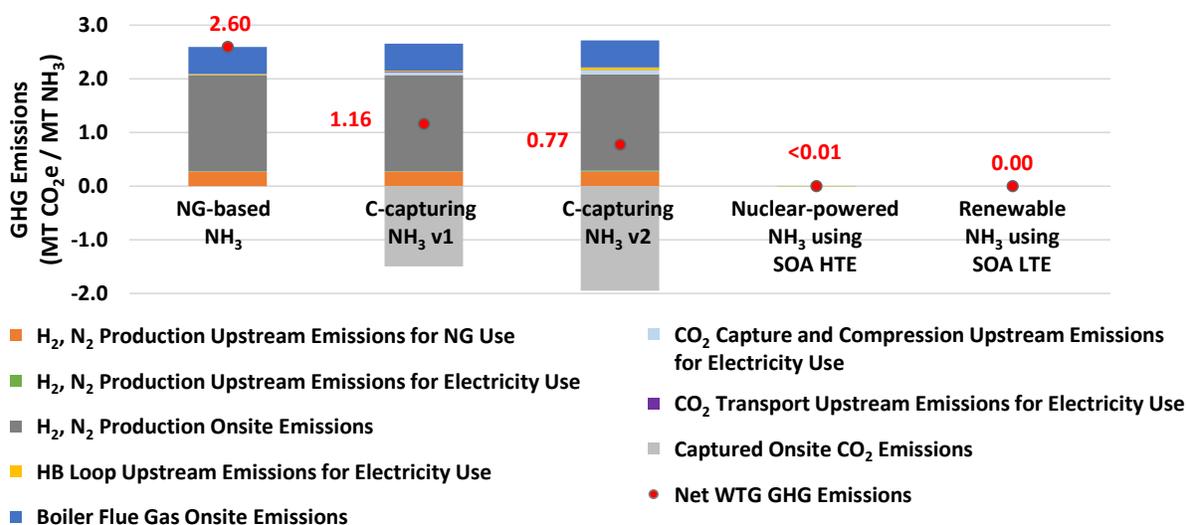
Fig. 8 GHG emissions of NG-based, carbon-capturing, nuclear-powered, and renewable ammonia production. Captured CO_2 emissions are shown as negative values. Net well-to-plant-gate (WTG) GHG emissions are shown as red dots. Nuclear-powered and renewable ammonia production assumes nuclear energy and renewable energy, respectively, used for all processes including water electrolysis, air separation, and Haber-Bosch.

most dominant cost factor for this LCOA is NG feedstock costs. The LCOA of NG-based ammonia in this study is smaller than the reported values from other studies. This is because, as described previously, this work employed the cheaper NG price from the AEO 2021 data, which corresponds to $4.24/MMBtu–LHV of NG. Fig. 7(a) compares the LCOAs of NG-based ammonia from multiple studies[3,9,44,45] that employed different NG prices. If a higher NG price — $5.79/MMBtu–LHV of NG (the U.S. price of NG in 2014[41]), for instance — is employed for this work, the LCOA of NG-based ammonia in this work increases to $339/MT of NH_3, which is consistent with the reported values from other studies that employed a similar range of NG prices.

In this work, two versions of carbon-capturing ammonia production were considered. As described previously, sensitivity analyses were performed for 100 to 1,000 miles of CO_2 pipeline transport distances and $35 to $50/MT CO_2 of Section 45Q carbon capture tax credits. The baseline LCOAs of carbon-capturing ammonia versions 1 and 2 are calculated to be $313 and $372 per MT of NH_3, respectively, when the tax credits are not considered. The baseline LCOAs of carbon-capturing ammonia versions 1 and 2 are decreased to $250 and $289 per MT of NH_3, respectively, when the tax credits are accounted for. The increase in LCOA of carbon-capturing ammonia version 1 compared to that of NG-based ammonia is mainly due to additional electricity consumption for the compression of captured process CO_2, which is represented by the increase in other variable costs, as well as CO_2 pipeline transportation costs.

Carbon-capturing ammonia production version 2 captures combustion CO_2 emissions using the Cansolv process. As shown in Fig. 6, the capital cost of carbon-capturing ammonia version 2 has doubled compared to that of NG-based ammonia. This is because the capital cost for the Cansolv process is high.

We investigated the LCOAs of nuclear-powered or renewable ammonia production for four scenarios of clean hydrogen production costs. The variation of clean H_2 production costs using SOA LTE and SOA HTE is accounted for through sensitivity analysis. When SOA LTE and SOA HTE technologies are considered, the baseline LCOAs of renewable and nuclear-powered ammonia were calculated to be $1,055 and $918 per MT of NH_3, respectively. As shown in Fig. 6, clean H_2 feedstock costs are the key cost driver for the renewable and nuclear-powered NH_3 LCOA. Therefore, for renewable and nuclear-powered ammonia production to be cheaper, low-cost clean hydrogen production is needed.

Fig. 7(b) shows the breakdown costs of clean hydrogen production through SOA LTE and SOA HTE. For both electrolysis technologies, electricity price, which is assumed to be $0.07/kWh, contributes the most to the total clean H_2 production costs. Therefore, to achieve the DOE 2020 target price, the electricity price needs to be cheaper than it currently is. In this work, if we consider the DOE 2020 target price ($2.00/kg H_2), the LCOA of nuclear-powered or renewable ammonia can decrease to $475/MT of NH_3, which is still more expensive than those of NG-based and carbon-capturing ammonia production. However, if the long-term target H_2 price ($1.00/kg H_2) is considered, the LCOA of nuclear-powered or renewable ammonia is calculated to be $270 per MT of NH_3, which is comparable to those of NG-based and carbon-capturing ammonia.

As compared to the conventional NG-based ammonia production cost of $229/MT NH_3, the clean H_2 breakeven price for nuclear-powered or renewable ammonia production is calculated to be $0.80/kg H_2 when the current electricity price of $0.07/kWh is considered. If we consider a cheaper electricity price of $0.03/kWh, the clean H_2 breakeven price is increased to $0.89/kg H_2.

LCA results
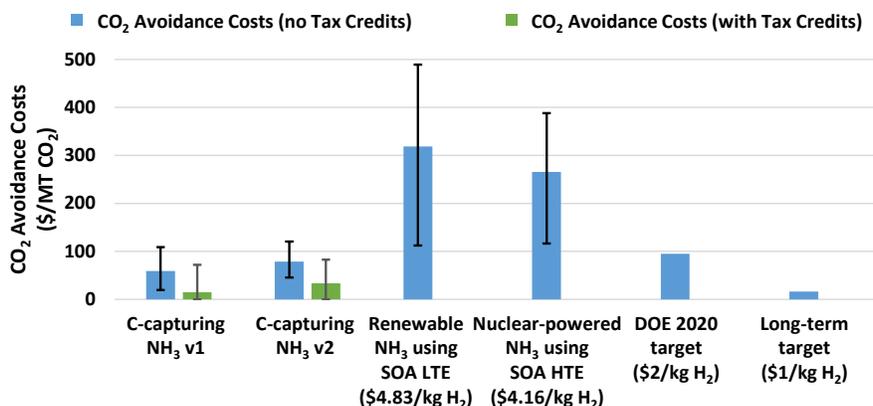
Fig. 9 CO_2 avoidance costs for carbon-capturing, nuclear-powered, and renewable ammonia production. Error bars for carbon-capturing ammonia are attributed to the sensitivity analyses for 100 to 1,000 miles of CO_2 pipeline transport distances and \$35 to \$50 per MT CO_2 of carbon capture tax credits. Error bars for renewable and nuclear-powered NH_3 are attributed to the variation of clean H_2 production costs. DOE 2020 and long-term target cases represent nuclear-powered or renewable ammonia production costs using the DOE 2020 and long-term target costs of clean H_2, respectively.

Fig. 8 illustrates the GHG emissions of NG-based, carbon-capturing, nuclear-powered, and renewable ammonia production. In the conventional NG-based ammonia production system, the purge gas stream contains CH_4, which is combusted in the boiler. Additional NG fuel is combusted in the boiler to provide sufficient heat for SMR. Accordingly, the conventional system has large CO_2 emissions from combusting a large amount of CH_4 (0.50 MT CO_2 per MT NH_3). The conventional system also has GHG emissions from the aMDEA process. Total onsite GHG emissions for the conventional system are calculated to be 2.30 MT CO_2e per MT NH_3. If the emissions from the upstream processes (i.e., NG production and electricity generation) are considered,[42] the WTG GHG emissions for producing 1 MT of NH_3 are estimated to be 2.60 MT CO_2e, which is comparable to the previous result (2.55 MT CO_2e/MT NH_3).[7]

For carbon-capturing ammonia version 1, 1.49 MT of process CO_2 emissions from the aMDEA process are captured, compressed, and transported via pipelines for CO_2 use such as CO_2-EOR. This portion is shown as a negative value in Fig. 8. Net WTG GHG emissions for carbon-capturing ammonia version 1 are calculated to be 1.16 MT CO_2e/MT NH_3. Carbon-capturing ammonia production version 2 captures 0.45 MT of combustion CO_2 emissions using the Cansolv process, as well as 1.49 MT of the process CO_2 emissions. In this case, net WTG GHG emissions are reduced to 0.77 MT CO_2e/MT NH_3.

In the nuclear-powered or renewable ammonia production system, the flue gas from the boiler does not contain any GHG, because the system does not employ any carbon material. We assumed clean hydrogen is produced using nuclear power or a renewable source of electricity for nuclear-powered or renewable ammonia production, respectively. Clean H_2 produced via HTE using solid oxide electrolyzer and nuclear power have 0.12 kgCO_2e/kg H_2 of GHG emissions.[42] Also, electricity generated from nuclear power shows 0.002 kgCO_2e/MJ of GHG emissions.[42] Therefore, WTG GHG emissions of nuclear-powered ammonia production are calculated to be less than 0.01 MT CO_2e per MT NH_3. WTG GHG emissions of renewable ammonia is zero since it uses zero carbon electricity such as solar and wind power.

CO_2 avoidance cost results

CO_2 avoidance costs for carbon-capturing and nuclear-powered/renewable ammonia production are calculated as shown in Fig. 9. For both versions of carbon-capturing ammonia production, their CO_2 avoidance costs are heavily dependent on the CO_2 pipeline transport distance. If CO_2 is transported a short distance of 100 miles, carbon-capturing ammonia versions 1 and 2 need only \$19.6 and \$45.3 to avoid 1 MT of CO_2 emissions, respectively, when carbon capture tax credits are not considered. However, if CO_2 needs to be transported 1,000 miles, \$109.0 and \$120.4 are required for carbon-capturing ammonia versions 1 and 2, respectively, to avoid 1 MT of CO_2 emissions when there are no carbon capture tax credits. For the baseline pipeline transport distance of 500 miles, CO_2 avoidance costs for carbon-capturing ammonia versions 1 and 2 are calculated to be \$59.1 and \$78.7 per MT of CO_2 emissions.

When 45Q carbon capture tax credits are included, CO_2 avoidance costs for carbon-capturing ammonia versions 1 and 2 are decreased to \$14.8 and \$33.3 per MT of CO_2 emissions, respectively, for the baseline pipeline transport distance. If the CO_2 pipeline transport distance is short (less than 250 miles for carbon-capturing ammonia version 1, for example) and the tax credits are considered, zero avoidance cost is needed for carbon-capturing ammonia since its LCOA can be cheaper than that of conventional NG-based ammonia.

CO_2 avoidance costs for nuclear-powered or renewable ammonia highly depend on the clean H_2 production costs as shown in Fig. 9. If we consider the baseline clean H_2 production costs of \$4.83 and \$4.16 per kg of H_2 using SOA LTE and HTE technologies, respectively, their CO_2 avoidance costs are much more expensive than those for carbon-capturing ammonia due to the high production costs of clean H_2.

If clean H_2 production cost can be as cheap as \$2.00/kg H_2 (DOE 2020 target price), the CO_2 avoidance cost decreases to \$94.9/MT CO_2, which is still more expensive than the baseline CO_2 avoidance costs for carbon-capturing ammonia production. If \$1.00/kg H_2 of clean hydrogen production cost is achieved, only \$16.0/MT CO_2 of CO_2 avoidance cost is required for nuclear-powered and renewable ammonia production.

Conclusions

Ammonia is produced from hydrogen and nitrogen through the HB process. For conventional ammonia production, hydrogen is produced via SMR and WGS processes, and nitrogen is provided by combusting oxygen in the air. Alternatively, hydrogen and nitrogen can be produced through water electrolysis and cryogenic air separation, respectively.

In this work, we developed detailed engineering models of NG-based, carbon-capturing, and nuclear-powered/renewable ammonia production. TEA and LCA were conducted to calculate the LCOA and life cycle GHG emissions, respectively, based on the mass and energy balance results from the engineering models. Carbon-capturing ammonia can reduce the carbon intensity of ammonia production by capturing CO_2 emissions and transporting the captured CO_2 via pipelines for various CO_2 utilization applications such as CO_2-EOR. However, the production costs of carbon-capturing ammonia were higher compared to NG-based ammonia because carbon-capturing ammonia requires additional equipment for CO_2 capture, compression, and transport.

Nuclear-powered and renewable ammonia showed less nonrenewable energy demand and nearly eliminates WTG GHG emissions compared to NG-based ammonia. However, the production costs of nuclear-powered and renewable ammonia were much higher than those of NG-based and carbon-capturing ammonia when SOA electrolysis technologies were employed, because the clean H_2 price was identified as a key cost driver to the levelized costs of nuclear-powered and renewable ammonia. In addition, we examined the value of avoided CO_2 emissions for employing carbon-capturing, nuclear-powered, and renewable ammonia. For nuclear-powered and renewable ammonia to be cost-competitive, a much cheaper clean hydrogen production cost, such as \$1/kg H_2, is needed.

This work investigated techno-economic performances and life cycle impacts of conventional and alternative ammonia production pathways in the United States. Alternative production pathways could rely on various regional characteristics, such as future market demands and renewable energy availability. Therefore, a regional analysis could be conducted to assess techno-economic performances and life cycle emissions of various ammonia production technologies.

Conflicts of interest

There are no conflicts to declare.

Acknowledgements

References

1   International Energy Agency (IEA), Global demand for pure hydrogen, 1975-2018, https://www.iea.org/data-and-statistics/charts/global-demand-for-pure-hydrogen-1975-2018.

2   S. P. S. Giddey, S. Badwal, C. Munnings and M. Dolan, *ACS Sustain. Chem. Eng.*, 2017, **5**, 10231–10239.

3   S. A. Nosherwani and R. C. Neto, *J. Energy Storage*, 2021, **34**, 102201.

4   U.S. Geological Survey (USGS), Nitrogen Statistics and Information, https://www.usgs.gov/centers/nmic/nitrogen-statistics-and-information.

5   Food and Agriculture Organization (FAO), *World fertilizer trends and outlook to 2022*, Rome, Italy, 2019.

6   International Energy Agency (IEA), *Technology Roadmap - Energy and GHG Reductions in the Chemical Industry via Catalytic Processes*, 2013.

7   X. Liu, A. Elgowainy and M. Wang, *Green Chem.*, 2020, **22**, 5751–5761.

8   R. M. Nayak-Luke and R. Bañares-Alcántara, *Energy Environ. Sci.*, 2020, **13**, 2957–2966.

9   H. Zhang, L. Wang, J. Van herle, F. Maréchal and U. Desideri, *Appl. Energy*, 2020, **259**, 114135.

10   O. Osman, S. Sgouridis and A. Sleptchenko, *J. Clean. Prod.*, 2020, **271**, 121627.

11   C. Arnaiz del Pozo and S. Cloete, *Energy Convers. Manag.*, 2022, **255**, 115312.

12   F. Y. Al-Aboosi, M. M. El-Halwagi, M. Moore and R. B. Nielsen, *Curr. Opin. Chem. Eng.*, 2021, **31**, 100670.

13   G. Jeerh, M. Zhang and S. Tao, *J. Mater. Chem. A*, 2021, **9**, 727–752.

14   Aspen Technology, *Aspen Plus Ammonia Model*, 2015.

15   J. Y. Mak, S. Mokhatab and W. A. Poe, in *Handbook of Natural Gas Transmission and Processing (Third Edition): Principles and Practices*, Gulf Professional Publishing, 2015, pp. 123–135.

16   M. Appl, in *Ullmann's Encyclopedia of Industrial Chemistry*, 2011.

17   H. Ebrahimi, A. Behroozsarand and A. Zamaniyan, *Chem. Eng. Res. Des.*, 2010, **88**, 1342–1350.

18   W. H. Chen, M. R. Lin, T. L. Jiang and M. H. Chen, *Int. J. Hydrogen Energy*, 2008, **33**, 6644–6656.

19   U.S. Environmental Protection Agency (EPA), *AP 42, Fifth Edition, Volume I Chapter 8: Inorganic Chemical Industry*, 1993.

20   V. Feyzi, M. Beheshti and A. Gharibi Kharaji, *Energy*,

2017, **118**, 77–84.

21   B. Zhao, F. Liu, Z. Cui, C. Liu, H. Yue, S. Tang, Y. Liu, H. Lu and B. Liang, *Appl. Energy*, 2017, **185**, 362–375.

22   L. Tao and R. Davis, NREL 2017 Biochemical Sugar Model, https://www.nrel.gov/extranet/biorefinery/aspen-models/.

23   G. Zang, P. Sun, A. A. Elgowainy, A. Bafana and M. Wang, *J. CO2 Util.*, 2021, **46**, 101459.

24   P. Spath, A. Aden, T. Eggeman, M. Ringer, B. Wallace and J. Jechura, *Biomass to Hydrogen Production Detailed Design and Economics Utilizing the Battelle Columbus Laboratory Indirectly-Heated Gasifier*, 2005.

25   F. Abdollahi, I. G. C. Craig and M. Neisiani, *Energy Procedia*, 2017, **114**, 6266–6271.

26   R. E. James III, D. Kearins, M. Turner, M. Woods, N. Kuehn and A. Zoelle, *Cost and Performance Baseline for Fossil Energy Plants Volume 1: Bituminous Coal and Natural Gas to Electricity*, 2019.

27   M. D. Jensen, S. M. Schlasner, C. D. Gorecki and N. Wildgust, *Opportunities and Challenges Associated with CO_2 Compression and Transport during CCS Activities*, 2017.

28   P. Shirley and P. Myles, *Quality Guidelines for Energy System Studies: CO_2 Impurity Design Parameters*, 2019.

29   Z. Abbas, T. Mezher and M. R. M. Abu-Zahra, *Int. J. Greenh. Gas Control*, 2013, **16**, 324–334.

30   W. M. Herron, Steve; Zoelle, Alexander; Summers, *Cost of Capturing CO_2 from Industrial Sources*, 2014.

31   D. Morgan and T. Grant, *FE/NETL CO2 Transport Cost Model (2018): Description and User's Manual*, 2018.

32   D. Peterson, J. Vickers and D. DeSantis, *Hydrogen Production Cost From PEM Electrolysis - 2019*, 2020.

33   D. Peterson, J. Vickers and D. DeSantis, *Hydrogen Production Cost From High Temperature Electrolysis – 2020*, 2020.

34   H.-W. Häring, in *Industrial Gases Processing*, Wiley-VCH Verlag GmbH & Co. KGaA, Weinheim, Germany, 2008, pp. 9–109.

35   E. Querol, B. Gonzalez-regueral, A. Ramos and J. L. Perez-benedito, *Energy*, 2011, **36**, 964–974.

36   M. Penev, G. Saur, C. Hunter and J. Zuboy, *H2A Hydrogen Production Model : Version 3 . 2018 User Guide*, 2018.

37   R. Turton, R. C. Bailie, W. B. Whiting and J. A. Shaeiwitz, *Analysis, synthesis and design of chemical processes*, Pearson Education, 2008.

38   Great Plains Institute, Primer: 45Q Tax Credit for Carbon Capture Projects, https://betterenergy.org/blog/primer-section-45q-tax-credit-for-carbon-capture-projects/.

39   Hydrogen and Fuel Cell Technologies Office, DOE Technical Targets for Hydrogen Production from Electrolysis, https://www.energy.gov/eere/fuelcells/doe-technical-targets-hydrogen-production-electrolysis.

40   Hydrogen and Fuel Cell Technologies Office, Hydrogen Shot, https://www.energy.gov/eere/fuelcells/hydrogen-shot.

41   U.S. Energy Information Administration (EIA), Annual Energy Outlook 2021, https://www.eia.gov/outlooks/aeo/.

42   Argonne National Laboratory (ANL), *Summary of Expansions and Updates in GREET 2020*, 2020.

43   V. Hacker and K. Kordesch, in *Handbook of Fuel Cells*, 2010.

44   ARPA-E, *Renewable Energy to Fuels Through Utilization of Energy Dense Liquids (REFUEL) Program Overview*, 2016.

45   M. Fasihi, R. Weiss, J. Savolainen and C. Breyer, *Appl. Energy*, 2021, **294**, 116170.